A Waveguide Integrated GaN Distributed Bragg Reflector Cavity Using Low Cost Nanolithography

S. Jia[1], E.Le.Boulbar[2], K.Balram[1], J.R. Pugh[1], T. Wang[3], D.W.E. Allsopp[2], P.A. Shields[2] and M.J. Cryan[1]

[1]Department of Electrical and Electronic Engineering, University of Bristol

[2]Department of Electrical and Electronic Engineering, University of Bath

[3]Department of Electronic and Electrical Engineering, University of Sheffield

simeng.jia@bristol.ac.uk, m.cryan@bristol.ac.uk

Abstract:

In this paper, we present the design, fabrication and measurement of gallium nitride (GaN) Distributed Bragg Reflector (DBR) cavities integrated with input and output grating couplers. The devices are fabricated using a new, low cost nanolithography technique: Displacement Talbot Lithography (DTL) combined with Direct Laser Writing (DLW) lithography. The finite difference time-domain (FDTD) method has been used to design all the components and measured and modelled results show good agreement. Such devices have applications in GaN integrated photonics and biosensing.

1. Introduction

GaN is a promising candidate for many integrated photonics applications [1-6]. It is transparent from ~400 nm to ~13.6 μm [7], has a relatively high refractive index of ~2.4 and is used as the basis for a range of visible LEDs and lasers [8-12]. These unique properties have been used in photonic integrated circuits and led to recent work developing GaN as a chemical and biological sensing platform [13]. GaN-based waveguides have achieved low loss [14,15] and have been implemented as freestanding waveguide structures [16-18]. GaN-based photonic crystal cavities have also been developed and high Q factors have been obtained which can be used to sense biological or chemical analytes [19,20]. Although the technology of GaN waveguides is not as mature as Silicon-on-Insulator [21], the characteristics of GaN discussed above act as an impetus to further explore photonic integrated circuits in this technology. The fabrication of GaN waveguides and photonic crystal cavities is almost always based on electron beam lithography. Although the accuracy of this method is very high, the manufacturing process is slow and is very expensive. This work aims to design a waveguide integrated GaN distributed Bragg reflector cavity using a new nanolithography technique: Displacement Talbot Lithography (DTL), which can produce large area, nanoscale periodic structures with low-cost and high-throughput [22, 23].

The proposed structure is shown in Figure 1, which includes two GaN gratings couplers and two GaN Distributed Bragg Reflector gratings forming a cavity. The use of DTL fabrication restricts the period of all gratings to be nominally the same across the whole wafer, with laser lithography being used to define the region where the gratings are present. In future structures it may be possible to have different etch depths for different gratings, but here we have restricted processing a single etch step. These limitations are not ideal for forming both grating couplers and DBR cavities, but compared to the very high cost of electron-beam lithography, DTL + DLW is an interesting much lower cost option and the paper shows the potential for this approach.

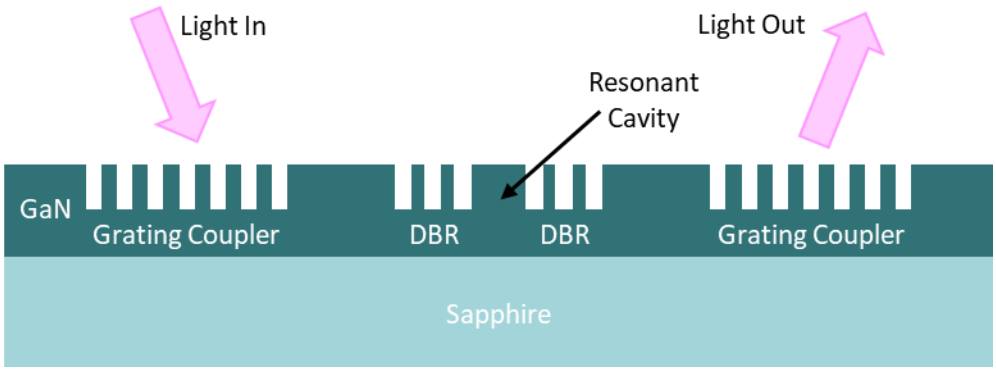

Figure 1: Schematic representation of proposed grating coupled DBR cavity

2. Grating Couplers

A. Modelling and design

We used the two-dimensional finite difference time-domain (FDTD) technique from Lumerical FDTD Solutions [24] to optimise the maximum out coupled power for a 1.5 µm layer of GaN-on-Sapphire. Figure 2 shows the 2D schematic cross-section for the in-out grating coupler structure.

In the model, a fundamental transverse electric (TE) mode source comes from a fibre which is single moded around the wavelength of interest which is 630-640 nm. This was initially based on the fact that a red laser would be used to show simple light coupling, this was eventually replaced with a supercontinuum laser source. Thus the fibre is a SMF600 with 125 µm cladding diameter and 4.3 µm core diameter. Light from the fibre will be diffracted into the reflected and transmitted orders. Some of the transmitted orders which satisfy the guided mode conditions can propagate in the 120 µm long waveguide and be coupled out into free space, then collected by an identical single mode fibre at the output. The simulation uses a wavelength range of 450 nm to 900 nm and is mainly focused on optimising across the 630-640 nm wavelength range. The gratings and waveguide are in the GaN layer with a refractive index n_{GaN}= 2.38 [25]. The substrate is sapphire with a refractive index $n_{Sapphire}$= 1.77 [26], and the cover region is air.

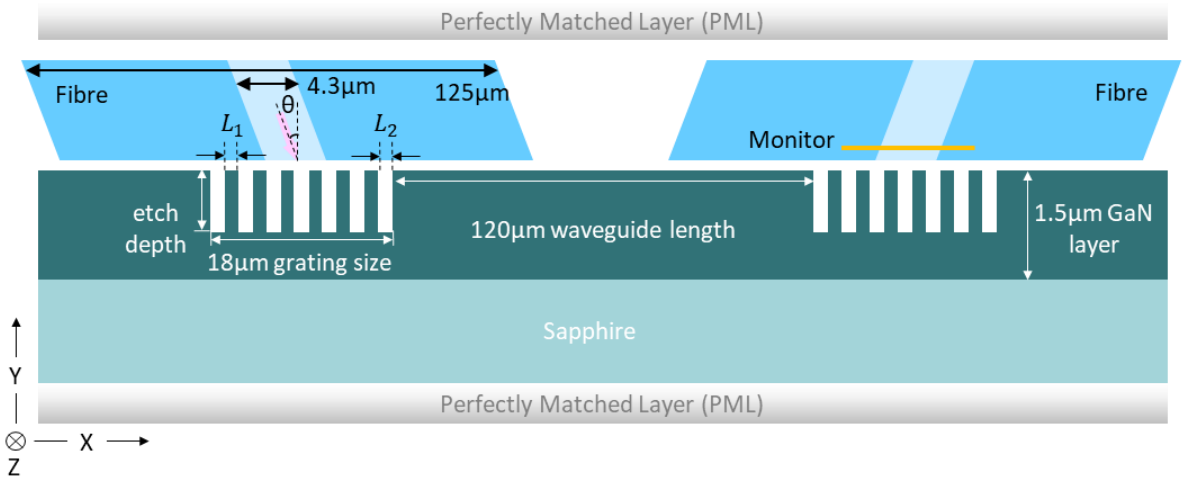

Figure 2: Geometry of 1.5 µm GaN on sapphire in-out grating couplers. Device parameters: n_{GaN} = 2.38, $n_{sapphire}$ = 1.77, grating period = $L_1 + L_2$ = 400 nm, filling factor = $L_1/(L_1 + L_2)$, grating length = 18 µm, number of periods = 45 waveguide length = 120 µm.

There are four main design parameters for the grating couplers: grating period, filling factor, etch depth and number of periods, where grating period $\Lambda = L_1 + L_2$ and filling factor a = L_1/Λ. In addition, the fibre angle of incidence plays an important role. In our case this was fixed at 15 ° based on the available optical measurement set up. The main design choice to be made is the grating period and diffraction theory can be used to determine the optimum value and this is simplest when the waveguide is single moded [27]. However, in our case the GaN slab waveguide is highly multimoded, supporting 8 TE modes around 630-640 nm wavelength. Thus in our case we based our choice on available DTL masks and decided on a 400 nm period grating. FDTD modelling was then used to determine the impact of etch depth and filling factor in order to guide the fabrication process. The number of periods was chosen as 45 giving a grating length of 18 µm which was felt to be sufficiently large with respect to the fibre core diameter of 4.3 µm. A waveguide length of 120 µm was chosen as a balance between simulation memory requirements and obtaining realistic results for waveguides that would be much longer in practice. In the FDTD modelling, by varying the etch depth ranging from 0 nm to 1500 nm and fill factor from 0.2 to 0.8, it was found that the TE0 mode input source has an optimum in-out transmittance at 640 nm wavelength when the fill factor is 0.45 and the etch depth is 600 nm. Figure 3 shows the transmittance spectra for the TE0 mode, TM0 mode and TE0+TM0 modes sources with these parameters. It can be seen that the TE0 mode has high transmission and the TM0 mode has very low transmission. This would allow us to use unpolarised light at the input and restrict the waveguide and cavity design to TE modes only. In the TE0 case, a number of peaks in transmittance are obtained in four wavelength regions: 480-530 nm, 610-660 nm, 660-720 nm and 720-780 nm. Here, the best transmittance is 0.109 or -9.65 dB at 634.5 nm wavelength. The bandwidth for this peak is about 10.5 nm. The transmittance of TM0 mode is almost zero, especially near the wavelength of 640 nm. In order to model the transmission of unpolarized light we can sum the TE and TM results as shown in the Figure 3.

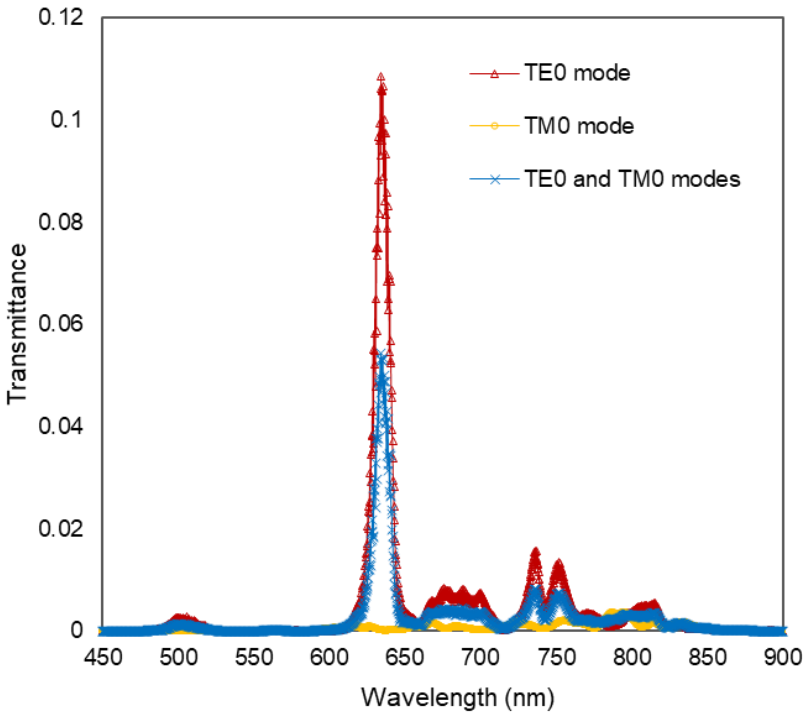

Figure 3: 2D FDTD modelling transmittance result for in-out coupling at 15 degree angle of incidence. Geometry of 1.5 µm GaN on sapphire in-out grating couplers. Device parameters: n_{GaN} = 2.38, $n_{sapphire}$ = 1.77, waveguide length = 120 µm, grating length = 18 µm, grating period = 400 nm, filling factor = 0.45, etch depth = 600 nm.

B. Fabrication

Since the process was to employ only a single GaN etch step using a 450-nm-thick PECVD SiNx hard etch mask, multiple lithography steps were required to pattern the SiNx mask beforehand. This is due to the different capabilities of the two lithography techniques: DTL can pattern periodic nanoscale features but only with large areas, whereas Direct Laser Writing can pattern arbitrary features >~1µm. Three different regions on the mask are required: large areas of SiNx to protect the waveguide, grating patterns for the couplers and the DBRs, and large unprotected areas in order to surround the waveguide.

The first step of the fabrication process was to define the large waveguide features in the mask. A S1813 positive photoresist mask was patterned via DLW (µPG 101, Heidelberg Instruments) and then transferred into the SiN_x via ICP etching using CHF_3 chemistry. This resist was then removed before applying a second, 350-nm-thick, high-resolution, AZ15NXT negative photoresist layer (on top of a Wide 8C bottom anti-reflective coating to improve resolution). This was exposed via DTL (PhableR 100C, EULITHA) to create a 400-nm-pitch grating in the resist across the whole sample area. A second exposure via DLW then fully exposed the negative resist in all areas where gratings were not required before CHF_3 plasma was used to transfer the resist pattern into the SiN_x. In this way, small grating regions could be created in the SiN_x whilst the negative resist protected the surrounding sample. The resist was subsequently removed.

The resulting SiN_x was used as a mask to etch ~780 nm of GaN using Cl_2/Ar plasma. A high etch temperature of 150 °C was used to ensure vertical sidewall etch profiles [28]. Finally, the SiN_x mask was stripped in HF-based solution.

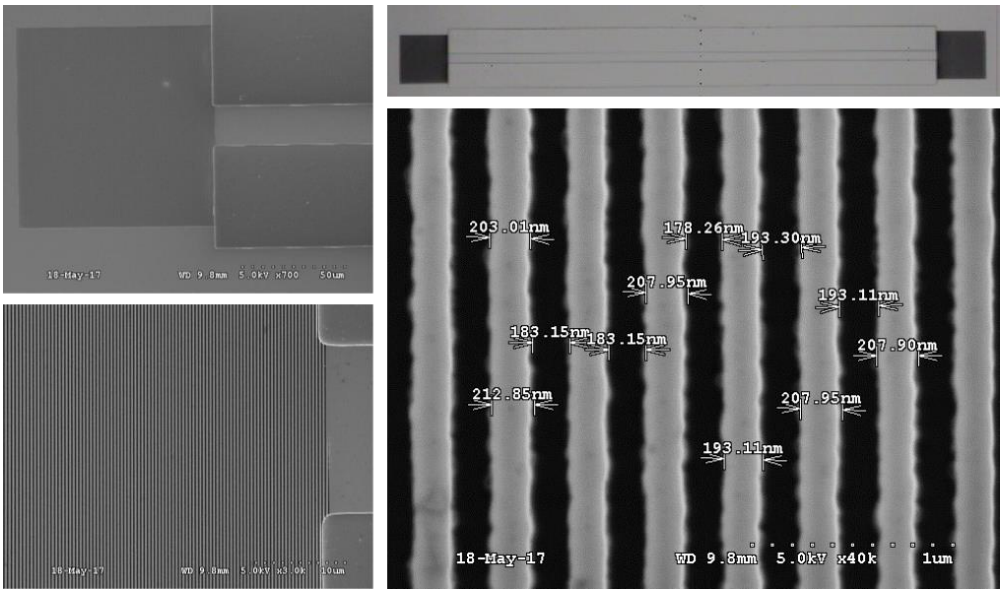

Figure 4: SEM images of typical grating couplers and waveguides after DTL and DLW processing

Figure 4 above shows SEM pictures of typical grating couplers. The filling factor is shown for one grating coupler and is seen to be close to 0.5. The etch depth has been estimated to be 780 nm. Figure 5 shows the simulated in-out transmittance for TE0 mode, TM0 mode and TE0+TM0 modes sources with these parameters. The figure shows that both TE0 mode and TM0 mode have good transmittance around 630-640 nm wavelength with these structural parameters. This will complicate the operation of the device; in future work we will use polarisation controllers to restrict measurement to a single polarisation, but here we will continue to use unpolarised light.

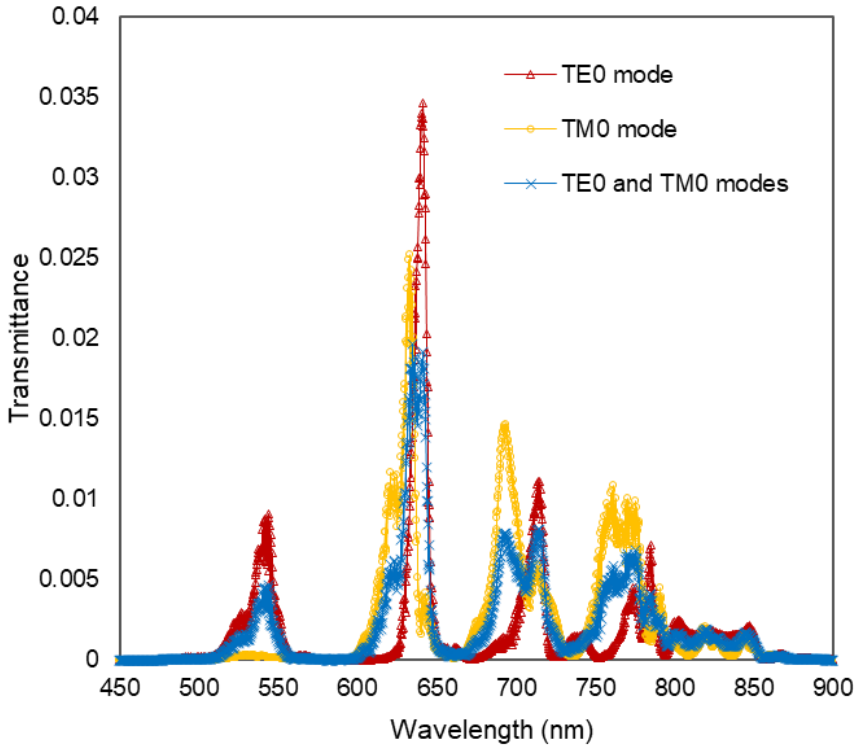

Figure 5: 2D FDTD modelling transmittance result for in-out coupling at 15 degree angle of incidence. Device parameters: n_{GaN} *= 2.38,* $n_{sapphire}$ *= 1.77, waveguide length = 120 μm, grating length = 18 μm, grating period = 400 nm, filling factor = 0.5, etch depth = 780 nm.*

C. Measurement

Optical testing was performed using the measurement setup shown in Figure 6. The chip is placed on a XYZ translation stage. Two single mode optical fibres (SMF600) are mounted at an angle of 15 ° which couple light into and out of the chip. A SuperK COMPACT supercontinuum laser delivers the unpolarized light to the input fibre. To avoid the possibility that direct coupling damages the fibre facet, two achromatic objectives are added to couple from laser into free-space, then into the fibre. An Ocean Optics spectrometer is used to collect in-out coupling intensity data. A high-magnification camera is used to show a plan-view and the location of fibres on the sample. The second camera shows a side-view to check the vertical distance between the fibre facets and sample.

The layout of part of the chip is shown in Figure 7. A series of 100 μm*100 μm area grating couplers with varying waveguide lengths are located in this area.

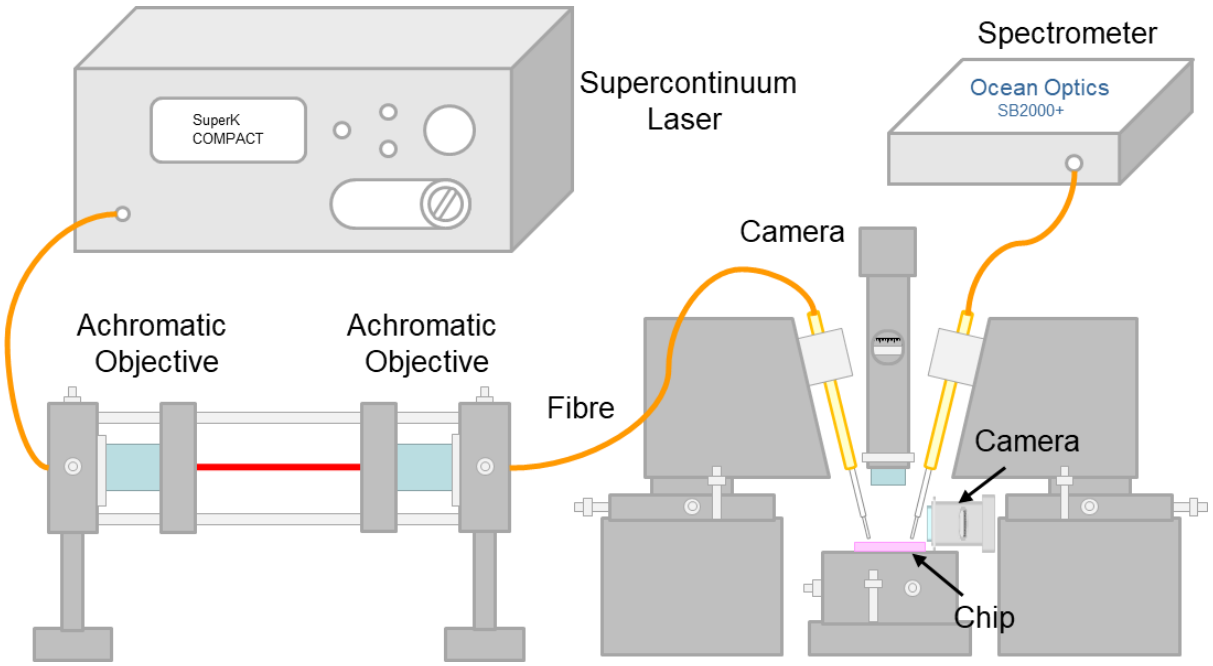

Figure 6: Fibre based measurement set up which includes a supercontinuum laser, two achromatic objectives, two single mode fibres, chip, detector and two cameras.

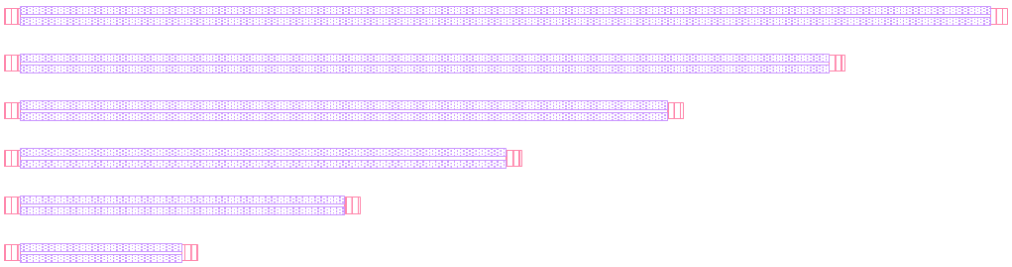

*Figure 7: The layout of part of the chip: grating couplers with straight waveguides. Device parameters:100 μm*100 μm grating couplers, grating period =400 nm, waveguide width = 20 μm, waveguide length from 1 mm to 6 mm (in steps of 1 mm)*

The plan view image of GaN grating couplers and waveguide is shown in Figure 8(a). The output grating can be seen to be bright in Figure 8(b) when the output fibre is removed, showing that reasonable coupling has been obtained.

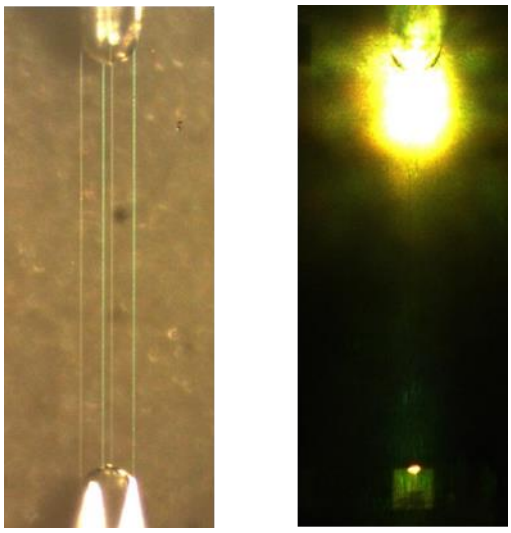

(a) (b)

Figure 8: Image of grating couplers with 1 mm waveguide plan-view. (a) In-out coupling setup plan-view; (b) Output grating is bright when the output fibre is removed.

The in-out coupling measurement results with varying waveguide length are shown in Figure 9(a). It can be seen that there are two regions of high transmittance around 640 nm and 700 nm and this matches up well with the TE0+TM0 mode result shown in Figure 5. There is some variation in the peak wavelength between the 6 waveguide lengths, but this is expected due to the fabrication differences between gratings in the different waveguides. In the case of the 1 mm waveguide there is a strong ripple with a peak spacing of 4.1 nm. It is believed that this ripple is related to mode beating [29] between the multiple modes that can propagate in the waveguide and the mode spacing is of the order that would be expected for this length of waveguide. The longer waveguides do not have such a prominent ripple, but these will have higher loss, and this will tend to suppress the mode beating effect.

The coupling loss and waveguide attenuation are estimated by the cutback method. In order to accurately calculate the coupling loss, the input fibre should be connected directly to the output to act as a reference, however in our current set up this was not possible. Thus in order to make an approximate estimate for coupling loss, a silver mirror placed in the position of the chip was used as a reference. This will significantly underestimate the coupling loss and in future work we will improve this coupling loss estimate. Figure 9(b) shows the transmittance at 639 nm normalized to the mirror transmittance for each waveguide length. In the case of the 1 mm length, due to the strong ripple an estimate was required which removed the effect of these ripples. The slope of the linear fit gives the waveguide loss to be 3.9 dB/mm. The coupling loss, compared to the mirror transmittance, is obtained as the intercept with the vertical axis and is found to be 2 dB in total or 1 dB per coupler.

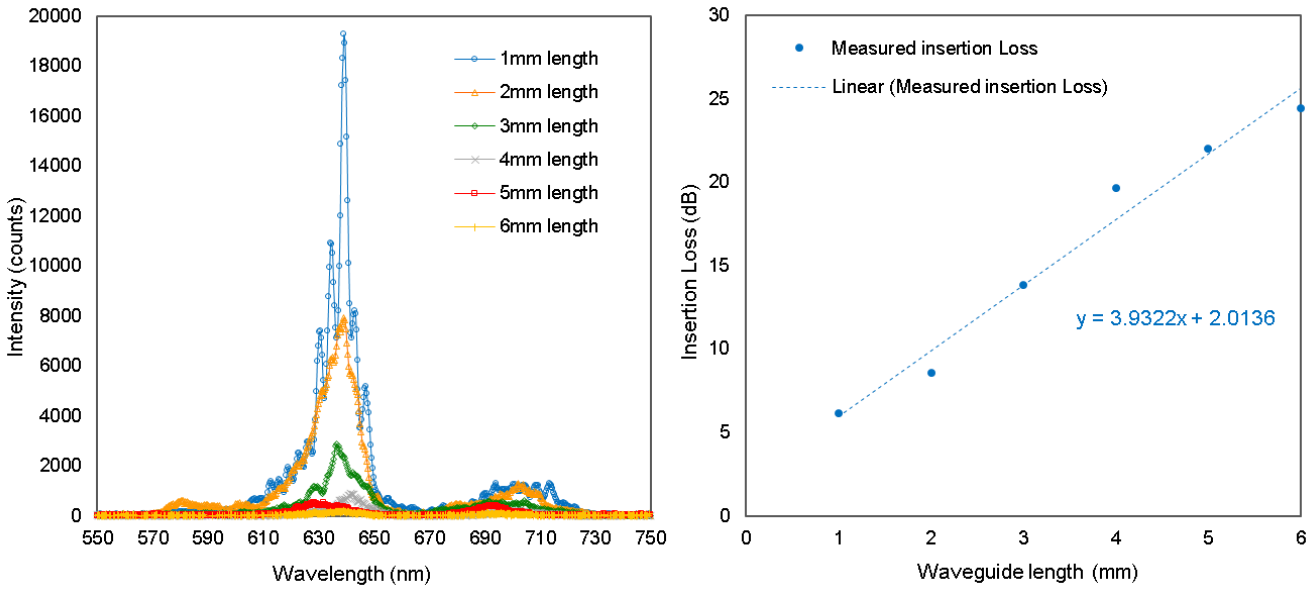

(a) (b)

Figure 9: (a) Measured output intensity for 20 μm width waveguide in-out coupling with varying waveguide lengths; (b) Coupling loss and waveguide attenuation estimation using the cut-back method.

3. DBR cavity

A. Modelling and design

Next, we focus on the DBR cavity design. The schematic representation of an isolated cavity is shown in Figure 10. It consists of two 400 nm period DBR gratings forming a cavity. As described above we represent unpolarised light with a TE0+TM0 mode source. The length of the cavity was chosen to be 8 μm, ensuring that there is sufficient length to observe resonant peaks, and the filling factor and etch depth remain unchanged at 0.5 and 780 nm, respectively.

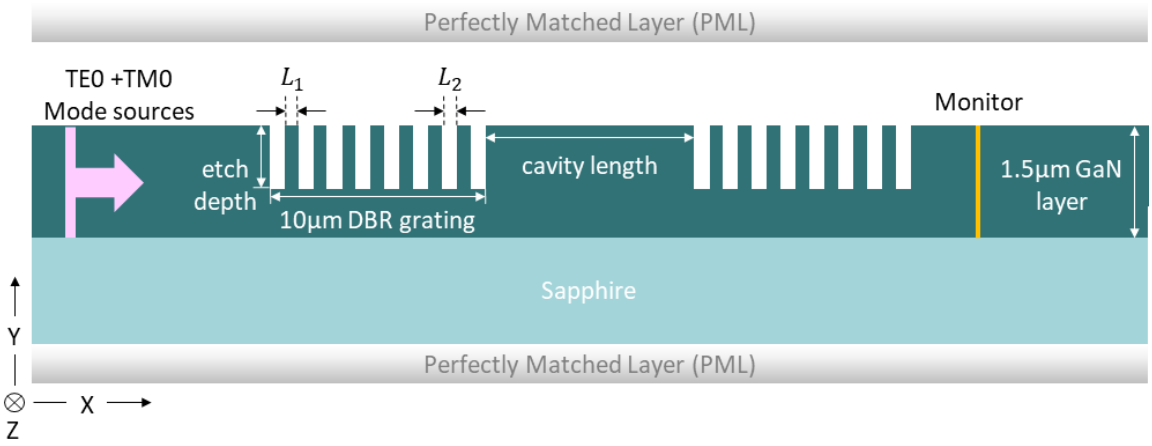

Figure 10: Geometry of two DBR gratings with 8 μm cavity. Device parameters: grating period = $L_1 + L_2$ = 400 nm, filling factor = $L_1/(L_1 + L_2)$ = 0.5, DBR grating size = 10 μm.

The modal transmittance of Figure 11 is for 25 period DBR gratings with an 8 μm cavity. A mode spacing of ~10 nm can be seen at an etch depth of 780 nm around 640 nm wavelength which will allow ~two resonant peaks to be observed in the

bandwidth of the grating coupler, shown in Figure 9. It can be seen that 780 nm etch depth is an optimum for resonant cavity behavior. If the grating is etched deeper then very little light is coupled into the cavity and the transmission drops rapidly. If the etching depth is less, then very little light is trapped in the cavity. In order to understand these effect further we can use FDTD to look at the fields at one of the resonant peaks for the 780 nm etch depth, shown in Figure 12.

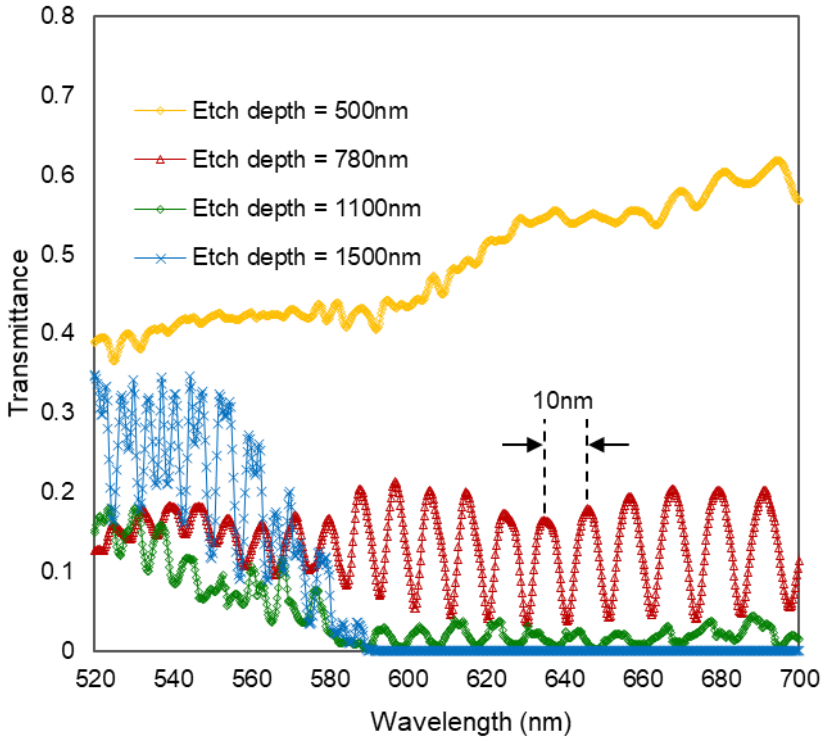

Figure 11: Simulated TE0+TM0 mode sources transmittance spectra of DBRs cavity with varying etch depth, filling factor = 0.5, cavity length = 8 μm.

Figure 12 show the magnitudes of the E_z field for TE0+TM0 modes with 780 nm etch depth at 637 nm wavelength which is one of the resonance peaks. Because the structure is not fully etched, some of the light propagates through the region beneath the Bragg grating and couples in to the cavity. It can be seen that since the waveguide is multimoded, very non-ideal operation is observed for this structure. In future work, thinner GaN layers and ridge waveguide structures will be used to ensure single mode operation which will simplify device operation significantly.

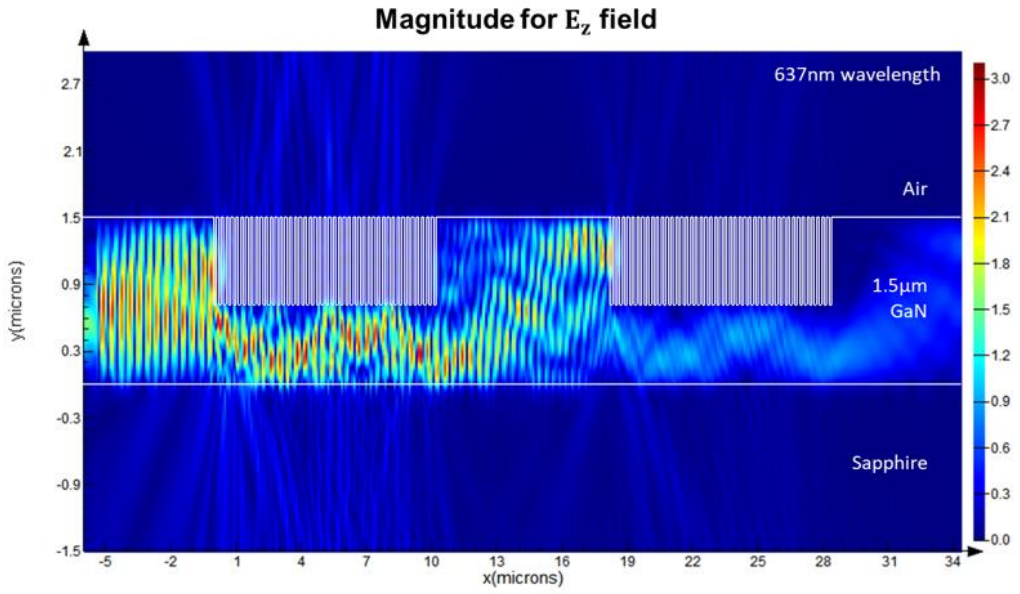

Figure 12: The E_z field distribution in cross section for the peak wavelength (637 nm), TE0+TM0 modes propagating from left to right. Grating parameters: filling factor = 0.5, period=400 nm, etch depth = 780 nm, cavity length = 8 µm. (Vertical and horizontal axes not to scale).

Figure 13 shows the layout for one DBR cavity on the chip and Figure 14 shows an SEM picture of a typical 10 µm long cavity. There are some unetched portions of the DBRs which will cause some differences between measured and modelled results.

*Figure 13: The layout of part of the chip: grating couplers with DBR cavity. Device parameters:100 µm*100 µm coupling grating size, DBR grating length = 10 µm, DBR grating width = 60 µm, grating period = 400 nm, cavity length = 8 µm, waveguide width = 20 µm, waveguide length =1 mm.*

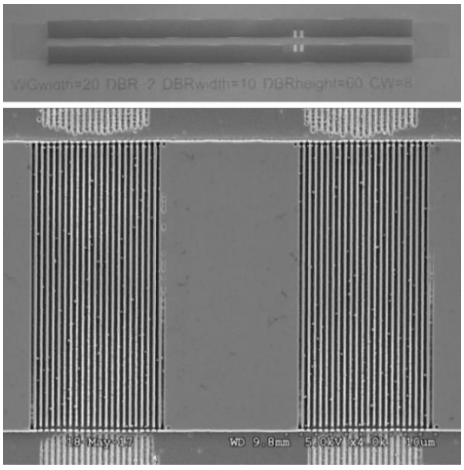

Figure 14: SEM image of a DBR resonant cavity

B. Measurement

The in-out coupling with DBR cavity measurement results are shown in Figure 15 for two different devices on the same chip and it can be seen that similar performance is obtained. The zoomed graphs are shown in Figure 16. It can be seen that a mode spacing of 10 nm is observed in one case, however not for the second device. Since the waveguide is highly multimoded, the mode spacing will depend on which modes are resonating in the cavity and the defects shown in Figure 14 will also produce non-ideal results. Insets show visible light camera images of both cavities which shows significant scattering from the first DBR and evidence of the high intensity peaks within the cavity.

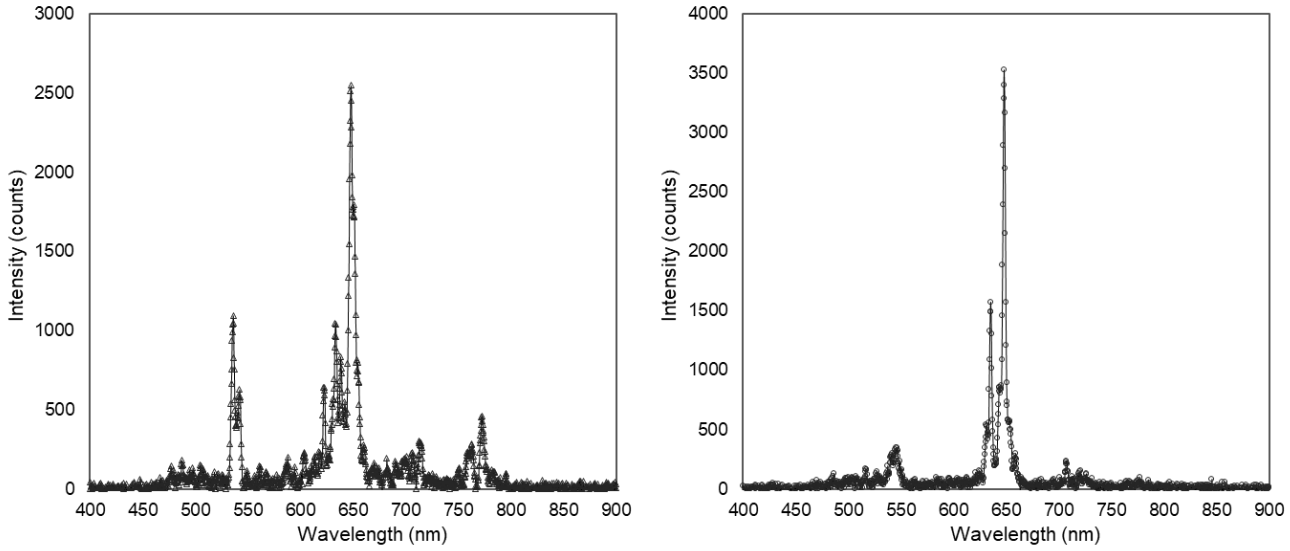

Figure 15: Measured in-out coupling with DBR cavities for two cavities on the same chip.

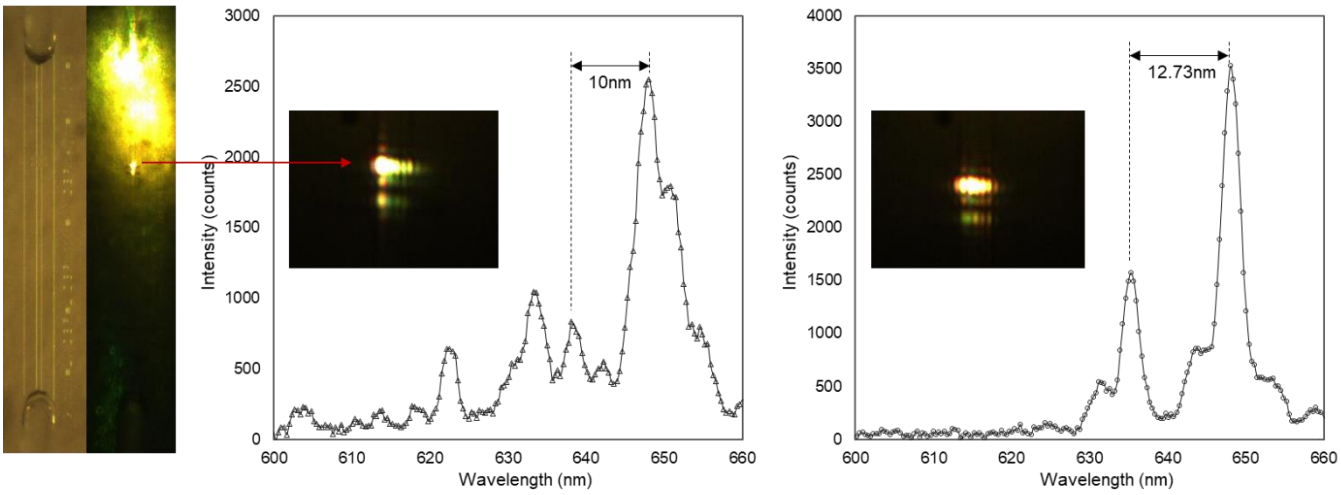

Figure 16: Zoom-in of measured in-out coupling for two different cavities and visible light images of light scattered from the cavities.

4. Conclusion

This paper has shown GaN DBR cavities with grating couplers fabricated using DTL. Cavities with Q factors of >200 have been measured which show the potential for this route to low cost commercial sensor applications. In future work single mode waveguides will be fabricated which will result in much more idealized grating coupler and cavity behavior which will lead to increased device performance. The main restriction for the DTL approach is that all gratings must have the same period, but with correct processing, different etch depths and fill factors could be obtained which would further improve the device performance.

Acknowledgements:

Engineering and Physical Sciences Research Council grant EP/M015181/1 www.manuGaN.org
We gratefully acknowledge Osram for the provision of the GaN/sapphire wafers.

Reference:

[1] Meier, C., Hennessy, K., Haberer, E.D., Sharma, R., Choi, Y.S., McGroddy, K., Keller, S., DenBaars, S.P., Nakamura, S. and Hu, E.L., 2006. Visible resonant modes in GaN-based photonic crystal membrane cavities. Applied physics letters, 88(3), p.031111.

[2] Tchernycheva, M., Messanvi, A., de Luna Bugallo, A., Jacopin, G., Lavenus, P., Rigutti, L., Zhang, H., Halioua, Y., Julien, F.H., Eymery, J. and Durand, C., 2014. Integrated photonic platform based on InGaN/GaN nanowire emitters and detectors. Nano letters, 14(6), pp.3515-3520.

[3] Choi, Y.S., Hennessy, K., Sharma, R., Haberer, E., Gao, Y., DenBaars, S.P., Nakamura, S., Hu, E.L. and Meier, C., 2005. GaN blue photonic crystal membrane nanocavities. Applied Physics Letters, 87(24), p.243101.

[4] Gromovyi, M., Semond, F., Duboz, J.Y., Feullet, G. and De Micheli, M., 2014. Low loss GaN waveguides for visible light on Si substrates. Journal of the European Optical Society: Rapid publications.

[5] Skorka, O., Salzman, J. and Zamir, S., 2003. Coupled waveguides in GaN-based lasers. JOSA B, 20(9), pp.1822-1828.

[6] Liu, Q., Wang, H., He, S., Sa, T., Cheng, X. and Xu, R., 2018. Design of micro-nano grooves incorporated into suspended GaN membrane for active integrated optics. AIP Advances, 8(11), p.115118.

[7] Chowdhury, A., Ng, H.M., Bhardwaj, M. and Weimann, N.G., 2003. Second-harmonic generation in periodically poled GaN. Applied physics letters, 83(6), pp.1077-1079.

[8] Ponce, F.A. and Bour, D.P., 1997. Nitride-based semiconductors for blue and green light-emitting devices. nature, 386(6623), p.351.

[9] Nakamura, S. and Fasol, G., 2013. The blue laser diode: GaN based light emitters and lasers. Springer Science & Business Media.

[10] Shchekin, O.B., Epler, J.E., Trottier, T.A., Margalith, T., Steigerwald, D.A., Holcomb, M.O., Martin, P.S. and Krames, M.R., 2006. High performance thin-film flip-chip InGaN–GaN light-emitting diodes. Applied Physics Letters, 89(7), p.071109.

[11] Teisseyre, H., Bockowski, M., Grzegory, I., Kozanecki, A., Damilano, B., Zhydachevskii, Y., Kunzer, M., Holc, K. and Schwarz, U.T., 2013. GaN doped with beryllium—An effective light converter for white light emitting diodes. Applied Physics Letters, 103(1), p.011107.

[12] David, A., Fujii, T., Moran, B., Nakamura, S., DenBaars, S.P., Weisbuch, C. and Benisty, H., 2006. Photonic crystal laser lift-off GaN light-emitting diodes. Applied physics letters, 88(13), p.133514.

[13] Wang, Y., Chen, J., Shi, Z., He, S., Garcia, M.L., Chen, L., Hueting, N.A., Cryan, M., Zhang, M. and Zhu, H., 2014. Suspended membrane GaN gratings for refractive index sensing. Applied Physics Express, 7(5), p.052201.

[14] Skorka, O., Meyler, B. and Salzman, J., 2004. Propagation loss in GaN-based ridge waveguides. Applied physics letters, 84(19), pp.3801-3803.

[15] Chen, H., Fu, H., Huang, X., Zhang, X., Yang, T.H., Montes, J.A., Baranowski, I. and Zhao, Y., 2017. Low loss GaN waveguides

at the visible spectral wavelengths for integrated photonics applications. Optics express, 25(25), pp.31758-31773.
[16] Liu, Q., Shi, Z., Zhu, G., Wang, W., Wang, Z. and Wang, Y., 2015. Freestanding GaN grating couplers at visible wavelengths. Journal of Optics, 17(4), p.045607.
[17] Sekiya, T., Sasaki, T. and Hane, K., 2015. Design, fabrication, and optical characteristics of freestanding GaN waveguides on silicon substrate. Journal of Vacuum Science & Technology B, Nanotechnology and Microelectronics: Materials, Processing, Measurement, and Phenomena, 33(3), p.031207.
[18] Vico Triviño, N., Dharanipathy, U., Carlin, J.F., Diao, Z., Houdre, R. and Grandjean, N., 2013. Integrated photonics on silicon with wide bandgap GaN semiconductor. Applied Physics Letters, 102(8), p.081120.
[19] Hueting, N.A. and Cryan, M.J., 2014. Doubly resonant photonic crystal cavities in gallium nitride for fluorescence sensing. JOSA B, 31(12), pp.3008-3017.
[20] Vico Triviño, N., Minkov, M., Urbinati, G., Galli, M., Carlin, J.F., Butté, R., Savona, V. and Grandjean, N., 2014. Gallium nitride L3 photonic crystal cavities with an average quality factor of 16 900 in the near infrared. Applied Physics Letters, 105(23), p.231119.
[21] Taillaert, D., Van Laere, F., Ayre, M., Bogaerts, W., Van Thourhout, D., Bienstman, P. and Baets, R., 2006. Grating couplers for coupling between optical fibers and nanophotonic waveguides. Japanese Journal of Applied Physics, 45(8R), p.6071.
[22] Chausse, P.J.P., Le Boulbar, E.D., Lis, S.D. and Shields, P.A., 2019. Understanding resolution limit of displacement Talbot lithography. Optics Express, 27(5), pp.5918-5930.
[23] Le Boulbar, E.D., Chausse, P.J.P., Lis, S. and Shields, P.A., 2017, June. Displacement Talbot lithography: an alternative technique to fabricate nanostructured metamaterials. In Nanotechnology VIII (Vol. 10248, p. 102480Q). International Society for Optics and Photonics.
[24] Lumerical-Solutions-Inc. (2014). Lumerical FDTD Solutions.
[25] Barker Jr, A.S. and Ilegems, M., 1973. Infrared lattice vibrations and free-electron dispersion in GaN. Physical Review B, 7(2), p.743-750.
[26] Malitson, I.H., 1962. Refraction and dispersion of synthetic sapphire. JOSA, 52(12), pp.1377-1379.
[27] Zhang, Y., McKnight, L., Engin, E., Watson, I. M., Cryan, M. J., Gu, E., ... & Dawson, M. D. (2011). GaN directional couplers for integrated quantum photonics. Applied Physics Letters, 99(16), 161119.
[28] Shields, P., Hugues, M., Zúñiga-Pérez, J., Cooke, M., Dineen, M., Wang, W., ... Allsopp, D. (2012). Fabrication and properties of etched GaN nanorods. Physica Status Solidi (C) Current Topics in Solid State Physics, 9(3-4), 631-634. https://doi.org/10.1002/pssc.201100394
[29] Dai, D., Tang, Y. and Bowers, J.E., 2012. Mode conversion in tapered submicron silicon ridge optical waveguides. Optics express, 20(12), pp.13425-13439.